Advances in Aircraft and Spacecraft Science, *Vol. 7, No. 5 (2020) 459-473*
DOI: https://doi.org/10.12989/aas.2020.7.5.459

Analysis of a shimming aircraft NLG controlled by the modified simple adaptive control

Andrea Alaimo and Calogero Orlando*

Faculty of Engineering and Architecture, Kore University of Enna, Cittadella Universitaria, 94100, Enna, Italy

(Received January 28, 2020, Revised March 25, 2020, Accepted March 26, 2020)

Abstract. The aircraft nose landing gear (NLG) can suffer of an unstable vibration called shimmy that is responsible of discomfort and of fatigue stress on the gear strut components. An adaptive controller is proposed in this paper to cope with the aforementioned problem. It is based on a method called Modified Simple Adaptive control (MSAC) which is able of governing the NLG motion by using a feedback signal that relies on just one output of the plant.
The MSAC only asks for the passivity of the controlled plant. With this aim, a parallel feedforward compensator is employed in this work to let the system satisfies the almost strictly passivity (ASP) requirements.
The nonlinear equations that govern the aircraft NLG shimmy vibration behavior are used to analyzed the controlled system transient response undergoing an initial disturbance and taking into account different taxiing speed values.

Keywords: shimmy; nose landing gear; modified simple adaptive control

1. Introduction

The possibility of realizing adaptive control system has attracted researchers since the early 50s.The reason of such interest mostly relies on the system capability to adapt to parameters change and on their ability to reject external disturbances or to cope with unmodeled dynamics, (ÅströmandWittenmark 2013). This has been particularly true in the aerospace framework where the possibility to quantify online the system uncertainties is useful to engender a control input capable to minimize the undesired disturbances avoiding the use of excessive actions to regulate the controlled dynamics, (Lavretsky and Wise 2013).

Among different adaptive control schemes, the modified simple adaptive one is investigated in the present work to suppress the nose landing gear shimmy vibration. The MSAC is a simplification of the Simple Adaptive Control that has been defined as a reduced order and stable direct model reference adaptive control, (Sobel *et al.* 1979, Barkana 2014). More in detail, the SAC only asks for an output feedback and, therefore, neither complete status feedback nor an online parameter estimate is required. A fictitious reference model, whose order doesn't depend on the plant order, generates a signal which is used to define the output tracking error. Such error allows to compute the input controlling signal along with a feedforward contribution obtained by taking advantage of the reference model input and state signals, (Barkana 2014). Recent

*Corresponding author, Professor, E-mail: calogero.orlando@unikore.it

http://www.techno-press.org/?journal=aas&subpage=7 ISSN: 2287-528X (Print), 2287-5271 (Online)

aeronautical applications of the SAC methodology can be found in the literature. Among others, (Andrievsky *et al.* 2019) have adopted SAC along with an Implicit Reference Model to ensure a smooth tracking of the roll angle to the requested path allowing the wing rock suppression; (Alaimo *et al.* 2019) have used a population decline swarm optimizer to optimally tune the controller parameters of a fault tolerant longitudinal flight control system; (Matsuki *et al.* 2018) have proposed a PID-SAC controller to lead the longitudinal and lateral motion of an aircraft and have tested experimentally its fault tolerant capability.

Starting from the consideration that the feedforward terms are not strictly needed to ensure the stability and convergence of the method, but just the output feedback is responsible of the asymptotic convergence of the tracking,(Barkana 2005),the SAC has been modified giving rise to the MSAC, Ulrich and de Lafontaine (2007).One of the main advantages of the MSAC is that it has a reduced number of invariant parameters to be tuned a priori, (Ulrich *et al.* 2012).The MSAC scheme is here applied to suppress the shimmy oscillation of an aircraft NLG.

The shimmy vibration is characterized by nonlinear oscillations of the NLG fork and wheel around the steering axis. Such oscillations are self-sustained and take energy from the friction tire-road interaction. The phenomenon is governed mostly by the advancing speed. In fact, as the taxiing speed becomes greater than a critical velocity value, the system behavior becomes unstable and the shimmy vibration onsets, (Somieski 1997). When the shimmy vibration starts, the amplitude of the fork-wheel rotation can increase at a very high rate causing not only discomfort to pilots and passenger but it can also lead strut elements to failure because of wearing phenomena and high fatigue stresses. It follows the need for shimmy vibration suppression that, generally, is obtained by opting for passive solutions, (Rahmani and Behdinan 2019).

However, the performance of passive shimmy dampers lowers when working out of the design condition and this has motivated several researches to look for active solutions. Only the output feedback ones are taken into consideration here. The reason is that output feedback approaches do not ask neither for the implementation of several sensors nor for state observer. This represents an advantage both in terms of sensors installation cost reduction and in terms of reduction of the online computational time used to adapt the scheme. To the best Author's knowledge only few works are present in literature that deal with output feedback scheme to suppress the shimmy oscillation. A controller based on anti-windup proportional integral derivative scheme has been employed and its stochastic robustness has been verified in the works of (Orlando and Alaimo2017, Alaimo *et al.* 2016). On the other hand, a fuzzy output feedback controller has been studied by (Pouly *et al.* 2008) to adaptively damp the shimmy vibration. The drawback of firsts is that the PID scheme is not adaptive while the latter has a too complicated and computational time demanding architecture. The proposed MSAC scheme can tackle both aforementioned drawbacks. The condition that is required is that the plant should be Almost Strictly Passive ASP, however, actual systems are not ASP. To solve such problem the system is augmented with a proper designed Parallel Feedforward Compensator PFC and the MSAC is applied to the augmented system, (Rusnak and Barkana 2009).

In this paper it is presented an adaptive shimmy damper based on the MSAC. The modified simple adaptive controller is first introduced in Section 2 along with the passivity conditions that the controlled system should satisfy. Then, in Section 3, the equations that govern the NLG shimmy behavior are given using the state space representation. The linearized transfer function model is also presented since it can easy the study the system passivity for SISO systems. Results are last presented and commented in Section 4 for a case of aeronautical interest.

2. Fundamentals of the simple adaptive controller

Let us assume that the plant can be described by the system

$$\begin{aligned}\dot{\mathbf{x}} &= \mathbf{A}\mathbf{x} + \mathbf{B}\mathbf{u} + \mathbf{d}\\ \mathbf{y} &= \mathbf{C}\mathbf{x}\end{aligned} \tag{1}$$

being **x** the n-dimensional state vector, **u** and **y** are the m-dimensional input and output vectors while **d** is a bounded disturbance vector that can be considered unknown and it is not needed by the adaptive SAC algorithm. **A**, **B** and **C** are the dynamic, input and output matrices, respectively. The SAC asks for the definition of a reference model that generates the signal $\mathbf{y_m}$ to be tracked by the output **y**. Let us define the model reference system as

$$\begin{aligned}\dot{\mathbf{x}}_m &= \mathbf{A}_m\mathbf{x}_m + \mathbf{B}_m\mathbf{u}_m\\ \mathbf{y}_m &= \mathbf{C}_m\mathbf{x}_m\end{aligned} \tag{2}$$

The vectors $\mathbf{u}_m$ and $\mathbf{y}_m$ are m-dimensional as well as **u** and **y** while no request is put on the dimension of the state vector $\mathbf{x}_m$. The SAC is designed to engender an adaptive control signal **u** such that the tracking error $\mathbf{e} = \mathbf{y} - \mathbf{y}_m$ vanishes and the closed loop system's signals remain bounded. In detail, the control input is written as

$$\mathbf{u} = \mathbf{K}_e\mathbf{e} + \mathbf{K}_x\mathbf{x}_m + \mathbf{K}_u\mathbf{u}_m \tag{3}$$

being

$$\begin{aligned}\mathbf{K}_\alpha &= \mathbf{K}_{\alpha P} + \mathbf{K}_{\alpha I}\\ \mathbf{K}_{\alpha P} &= \alpha\mathbf{\Gamma}_P\mathbf{r}\\ \dot{\mathbf{K}}_{\alpha I} + \eta\mathbf{K}_{\alpha I} &= \alpha\mathbf{\Gamma}_I\mathbf{r}\end{aligned} \tag{4}$$

with $\alpha = \{\mathbf{e}, \mathbf{x}_m, \mathbf{u}_m\}$. In Eq. (4), $\mathbf{\Gamma}_P$ and $\mathbf{\Gamma}_I$ are invariant gains to be defined *a-priori* while η is called forgetting terms and is introduced to avoid the divergence of the integral gains when disturbances are present (Barkana 2005).

The only condition that must be met is that the plant is Almost Strict Passive ASP. This means that the plant is stabilizable by a constant output feedback K^*; however, such output feedback gain is unknown and it is not to be implemented, (Barkana 2005). Moreover, the ASP condition implies that closed-loop system K^* meets the following relations

$$\begin{aligned}\mathbf{P}\left(\mathbf{A} - \mathbf{B}K^*\mathbf{C}\right) + \left(\mathbf{A} - \mathbf{B}K^*\mathbf{C}\right)^T\mathbf{P} &= -\mathbf{Q}\\ \mathbf{P}\mathbf{B} &= \mathbf{C}\mathbf{S}^T\mathbf{S}\end{aligned} \tag{5}$$

being **P** and **Q** positive definite matrices while $\mathbf{S}^T\mathbf{S}$ is positive definite and symmetric.

In particular, for a SISO system (as it is the case studied in the present work) the previous passivity conditions are met if, and only if, the plant transfer function $G(s)=\mathbf{C}(s\mathbf{I}-\mathbf{A})^{-1}\mathbf{B}$has relative degree $r=1$, all zeroes placed in the left complex plane and its numerator highest degree coefficient is positive, (Andrievsky 1994, Barkana 2005, Omori *et al.* 2013).

The issue arises considering that almost all real plants are not ASP. The strategy adopted to solve such problem consists in using a Parallel Feedforward Compensator PFC such that the augmented plant meets the ASP requirements (Barkana 1987). More in detail, the Parallel

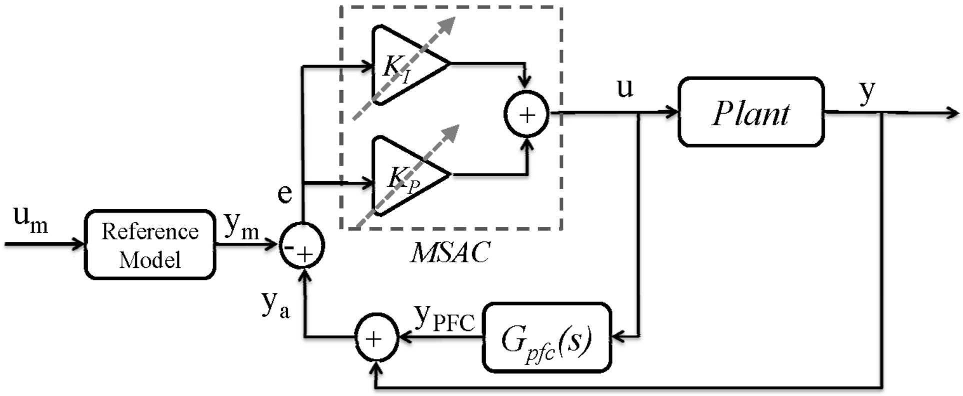

Fig. 1 Block diagram of PFC-MSAC controlled plant

Feedforward Compensator can be described as a LTI system

$$\begin{aligned} \dot{\mathbf{x}}_{pfc} &= \mathbf{A}_{pfc}\mathbf{x}_{pfc} + \mathbf{B}_{pfc}\mathbf{u} \\ \mathbf{y}_{pfc} &= \mathbf{C}_{pfc}\mathbf{x}_{pfc} \end{aligned} \tag{6}$$

Looking at Eq. (6) it is noted that the input of the PFC system is the control signal $\mathbf{u}$ while the PFC output vector is m-dimensional and summed to the plant output give rise to the augmented plant output $\mathbf{y}_a=\mathbf{y}+\mathbf{y}_{pfc}$. For a SISO linear system the augmented system can be easily written in terms of transfer function as $G_a(s)=G(s)+G_{pfc}(s)$. Once the augmented ASP system is built by using the PFC, the Simple Adaptive Controller is applied to the augmented plant to let $\mathbf{y}_a$ track $\mathbf{y}_m$. However, since the SAC scheme is now controlling the augmented system output, one of the design criteria of the PFC is that its static gain be as low as possible, obviously considering the physical realizability of the system.

Last, it is to be said that Ulrichand de Lafontaine (2007) proposed a further simplification of SAC starting from the consideration that only the $\mathbf{K}_{eI}$ term, see Eqs. 3-4, is mandatory to ensure the stability of the adaptive system. For the proof of system stability, the interested reader is referred to (Bar-Kana and Kaufman 1985). The MSAC algorithm is thus obtained from the SAC scheme by neglecting the adaptive gains $\mathbf{K}_x$ and $\mathbf{K}_u$ and retaining only $\mathbf{K}_e$. Moreover, for a SISO linear system Eqs. (3) and (4) become scalar with just $\alpha = \mathbf{e}$.

Fig. 1 graphically recalls aforementioned equations by using block diagram putting into evidence the MSAC block and that the parallel feedforward compensator modifies the definition of the tracking error to be zeroed.

3. MSAC shimmy damper

Fig. 1 shows the simplification of a nose landing gear used for shimmy modeling. Let us assume that the NLG is taxiing with constant speed V. The torque link connects the actuation system to the turning tube and the fork-wheel assembly. J is the system moment of inertia around the steering axis while e is the caster length. The kinematical variables that are used to write the system governing equations are the shimmy rotation ψ and the tire sideslip angle α. a and σ are the

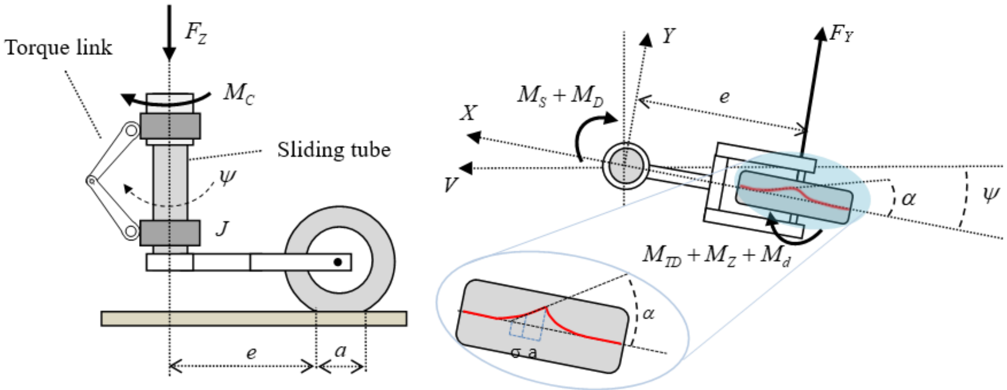

Fig. 2 Nose landing gear shimmy model

tire half contact and the relaxation lengths defined in accordance with the stretched string theory to model the tire deformation dynamic (Pacejka 2005).

M_C is the controlling torque generated by the MSAC while F_z is the aircraft weight that acts on the NLG. The stiffness and the damping moments introduced by the torque link and by the turning tube are M_S+M_D. On the other hand, the interaction between the tire and road engenders a damping tire moment M_{TD}, the self-aligning torque M_Z and the later force F_Y. In particular, the lateral force and the self-aligning moment depend nonlinearly on the tire sideslip angle through the following relationships

$$F_Y = \begin{cases} c_F \alpha F_z & |\alpha| \le \alpha_F \\ c_F \alpha F_z sign(\alpha) & |\alpha| > \alpha_F \end{cases} \tag{7}$$

$$M_Z = \begin{cases} c_M \dfrac{\alpha}{\pi} F_z \sin\left(\dfrac{\pi\alpha}{\alpha_M}\right) & |\alpha| \le \alpha_M \\ 0 & |\alpha| > \alpha_M \end{cases} \tag{8}$$

being c_F and c_M the cornering stiffness while α_F and α_M are limiting angles.

The equilibrium equation around the vertical axis and the stretched string model are the problem mathematical model that can be written in compact form by defining the state vector as $\mathbf{x} = \{\psi \quad \dot{\psi} \quad \alpha\}^T$ and using the state space representation. It reads as

$$\begin{aligned} \dot{\mathbf{x}}(t) &= \mathbf{A}\mathbf{x}(t) + \mathbf{b}u(t) + \mathbf{b}\left(M_d(t) + d_{\mathbf{x}}(\mathbf{x},t)\right) \\ y(t) &= \mathbf{c}^T \mathbf{x}(t) \end{aligned} \tag{9}$$

where the dynamic matrix is defined as

$$\mathbf{A} = \begin{bmatrix} 0 & 1 & 0 \\ -\dfrac{K_E}{J} & -\dfrac{1}{J}\left(K_D - \dfrac{\kappa}{V}\right) & -\dfrac{F_Z}{J}(c_M - e c_F) \\ \dfrac{V}{\sigma} & \dfrac{e-a}{\sigma} & -\dfrac{V}{\sigma} \end{bmatrix} \tag{10}$$

while the input and output vector write as

$$\mathbf{b}=\begin{bmatrix}0\\1\\0\end{bmatrix}; \qquad \mathbf{c}=\begin{bmatrix}1\\0\\0\end{bmatrix} \tag{11}$$

In Eq. (10), K_E is the NLG stiffness while K_D and κ are the NLG and tire-dynamic damping constants. The term $d_{\mathbf{x}}$ in Eq. (9) represents the nonlinear contribution introduced by the tire-road interaction and that is treated in the present study as a disturbance applied to the linearized model.

$$d_{\mathbf{x}}(\mathbf{x},t)=\frac{M_Z(\alpha)-eF_Y(\alpha)+F_Z(c_M-ec_F)\alpha}{J} \tag{12}$$

As it was stated before, to apply the MSAC approach it is not needed the knowledge of the disturbance inputs, but such disturbances must be bounded. Nonlinear actions are bounded and can thus be considered as disturbances in defining the MSAC parameters.

The problem is then linearized around the equilibrium state $\mathbf{x}_E=\mathbf{0}$. By using the mechanical parameters taken from (Orlando and Alaimo 2017), do not reported for the sake of conciseness, the following LTI state space model holds

$$\begin{gathered}\begin{Bmatrix}\dot\psi\\ \ddot\psi\\ \dot\alpha\end{Bmatrix}=\begin{bmatrix}0 & 1 & 0\\ -10^5 & -\left(10+\dfrac{270}{V}\right) & -36\times10^3\\ 3.33V & 0 & -3.33V\end{bmatrix}\begin{Bmatrix}\psi\\ \dot\psi\\ \alpha\end{Bmatrix}+\begin{Bmatrix}0\\1\\0\end{Bmatrix}u\\ y=\{1\quad 0\quad 0\}\begin{Bmatrix}\psi\\ \dot\psi\\ \alpha\end{Bmatrix}\end{gathered} \tag{13}$$

Observing Eq. (1)3 it can be seen that as the advancing velocity increases the NLG passive damping capability decreases and the time constant of the tire stretched string dynamic tends to reduces as well. On the contrary, as the taxiing speed reduces the uncontrolled system damping capability shows a hyperbolic growth. It is worth noting that the case V=0 is not of interest for the shimmy analysis as the shimmy oscillations start as soon as the taxiing speed becomes greater than a critical value named Shimmy Velocity V_S.

The other condition for the application of the MSAC scheme is that the input and output vectors have same dimension, which is equal to one in the present study case. It follows that the problem can be seen as a SISO linear system governed by transfer function that links the controlling moment to the shimmy angle ψ as

$$G(s)=\frac{V(3s+10V)}{3Vs^3+(10V^2+30V+810)s^2+(100V+302700)Vs+1360000V^2} \tag{14}$$

Observing Eq. (14) it stems that the system has one always negative zero and the numerator leading coefficient is positive but the relative degree is $r=2$, which means that the plant is not ASP. Thus, to apply the MSAC, a parallel feedforward compensator should be attached to the system.

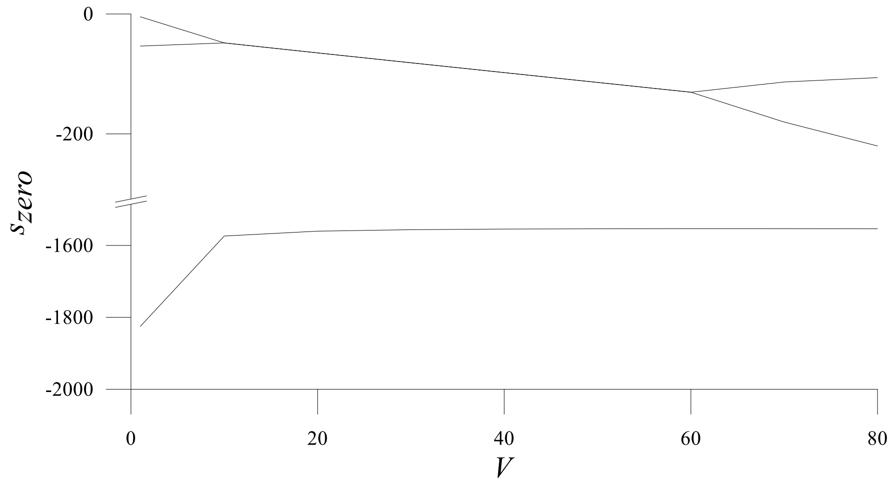

Fig. 3 Trend of the augmented plant zero points as function of velocity

According to (Barkana 2005), the PFC is designed as the inverse of an ideal proportional-derivative controller that stabilize *G(s)*. In the present work the PFC transfer function writes as

$$G_{pfc}\left(s\right)=\frac{160^{-1}}{10s+1} \tag{15}$$

and the augmented system transfer function reads as

$$G_a\left(s\right)=\frac{0.0019Vs^3+\left(0.0063V^2+3.0189V+0.5103\right)s^2+\left(10.063V+191.001\right)Vs+85.78}{3Vs^4+\left(10+30.3V+810\right)s^3+\left(101V^2+302703V+81\right)s^2+\left(1360010V+30270\right)Vs+136000V^2} \tag{16}$$

It is now evident that the relative degree of the augmented system transfer function is $r=1$ and that the numerator highest degree coefficient is positive. The last condition to be verified is that the zeroes of $G_a(s)$ have negative real part despite of the taxiing speed value. These have been computed for different values of advancing speed, ranging from 1 *m/s* to 80 *m/s*, and are shown in Fig. 3; it can be appreciated that all the zero points of the plant augmented by the PFC have negative real part. Then, it can be concluded that the augmented system meets the ASP requirements and the MASC can be applied.

The last element to be defined to apply the proposed adaptive controller is the Reference Model. It is to be recalled that the objective of the proposed adaptive controller is the damping of the shimmy oscillation and this means that the ideal reference output to be followed by the plant is $y_m=\psi=0$. Assuming a SISO LTI system as reference model it follows that $u_m=0$, as well justifying the application of the MSAC scheme instead of the complete SAC algorithm. It can be concluded that under the aforementioned working requirements the definition of the reference model is not necessary.

4. Numerical results

The NLG system is supposed to undergo an initial fork-wheel rotation disturbance while

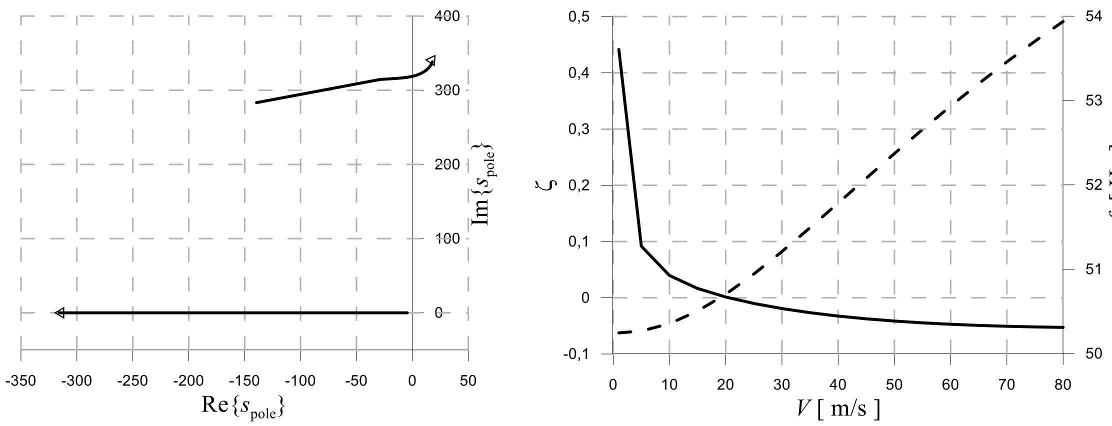

(a) Root locus (b) Modal damping and natural frequency

Fig. 4 System modal characteristics as function of speed

moving at constant speed. Different values of yaw angles and taxiing speed are considered to analyze the system response under different conditions. At first the response of the uncontrolled system is investigated, then the MSAC is introduced to study adaptively damped system behavior.

More in detail, the initial yaw angle is let vary between ψ_0={0.5,1, 2, 5} deg while the taxiing speed varies from 1 *m/s* to 80 *m/s* while the external disturbance torque is $M_d(t)=0$.

4.1 Uncontrolled system response

It is assumed that the controller is not present and, at first, the linearized plant eigenvalues s_{pole} are studied as function of taxiing speed to gain information about system stability and shimmy critical velocity. Fig. 4(a) shows the root locus graph evidencing the presence of one real negative eigenvalue and a pair of complex conjugate eigenvalues (only one is shown). The mode associated to the real pole is always stable despite of the taxiing speed value but the yawing shimmy mode associated to the complex conjugate pair becomes unstable as the advancing velocity increases. This confirms the existence of a critical speed value above which shimmy oscillation onsets. The trend of the yawing shimmy natural frequency and modal damping ratio are shown in Fig. 4(b). The first result to be outlined is that the damping ratio becomes negative, and the system response unstable, as the taxiing speed increases above the critical value V_s=20 m/s, indicating that the friction tire-road interaction is no more capable of withdrawing vibration energy from the system. On the other hand, it can be observed that the shimmy vibration frequency slightly rises from about 50 Hz to about 54 Hz.

The initial disturbance is then set to ψ_0=0.5 deg and the NLG speed transient response is studied by solving the nonlinear relationships Eq. (9). The taxiing speed is set to V_s=10 m/s and V_s=30 m/s to analyze the system behavior in its stable and unstable configurations. Results are shown in Fig. 5 in terms of fork-wheel rotation angle time history. It is visible that the system response is stable for $V<Vs$ and the shimmy oscillation is damped out in about 0.4 sec.

On the other hand, when the NLG velocity is greater than the critical one, the shimmy rotation ψ increases rapidly reaching a limit cycle oscillation (LCO) having amplitude ψ_{LCO}=25.8 deg.

The response of the system considering several velocity values are then considered. In

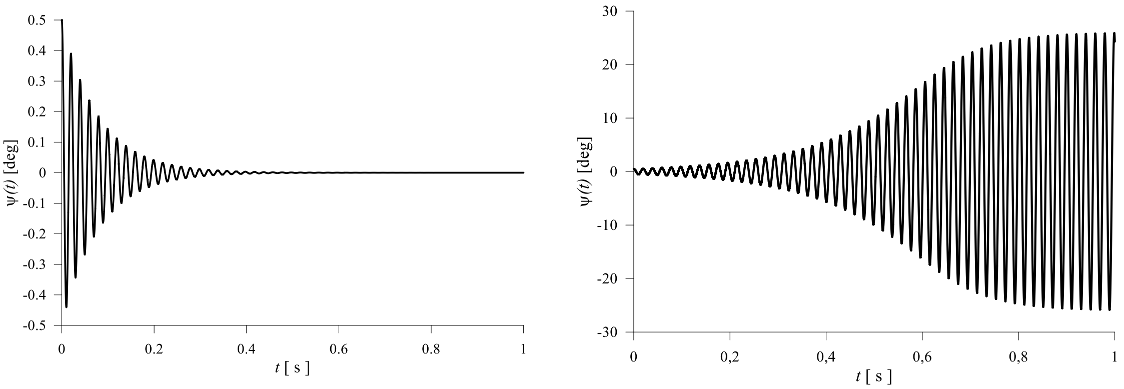

(a) ψ_0=0.5 deg, V=10 m/s (b) ψ_0=0.5 deg, V=30 m/s

Fig. 5 Uncontrolled system transient response

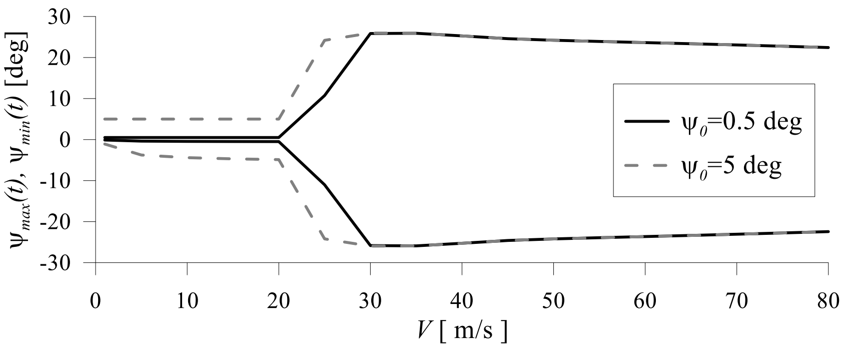

Fig. 6 Maximum open loop rotation

particular, the maximum and minimum shimmy rotation angles are computed and plotted in Fig. 6 taking into account two different initial yaw angle values, namely ψ_0=0.5 deg and ψ_0=5 deg. It appears form Fig. 6 that the maximum rotation value when V<20 is the initial disturbance but, as the taxiing speed rises above the critical shimmy velocity, the maximum rotation angle increases dramatically. Similar considerations stand for the minimum value of ψ(t). Observing the trend in Fig. 6, it stems that the system undergoing shimmy vibration reaches limit cycle oscillations whose amplitude increases from V=20 m/s to V=35 m/s then it reduces to about ψ=22.43 deg when the NLG advancing speed increases above 60 m/s. The effect of the initial disturbance amplitude is only confined to the velocity range V=20÷30 m/s, as ψ_0 increases the limit cycle oscillations amplitude raises.

4.2 MSAC controlled system response

To choose the adaption gains that allow to define the adaptation rules Eq. (4), it is considered that small adaptation parameters can results in a smooth transient behavior of the system but the drawback is that the tracking error may converge slowly. On the contrary, large adaptation gains may reduce the settling time but it can engender larger transient response (Ma *et al.* 2017). Because of the detrimental effects that the shimmy vibration can cause on the NLG structural

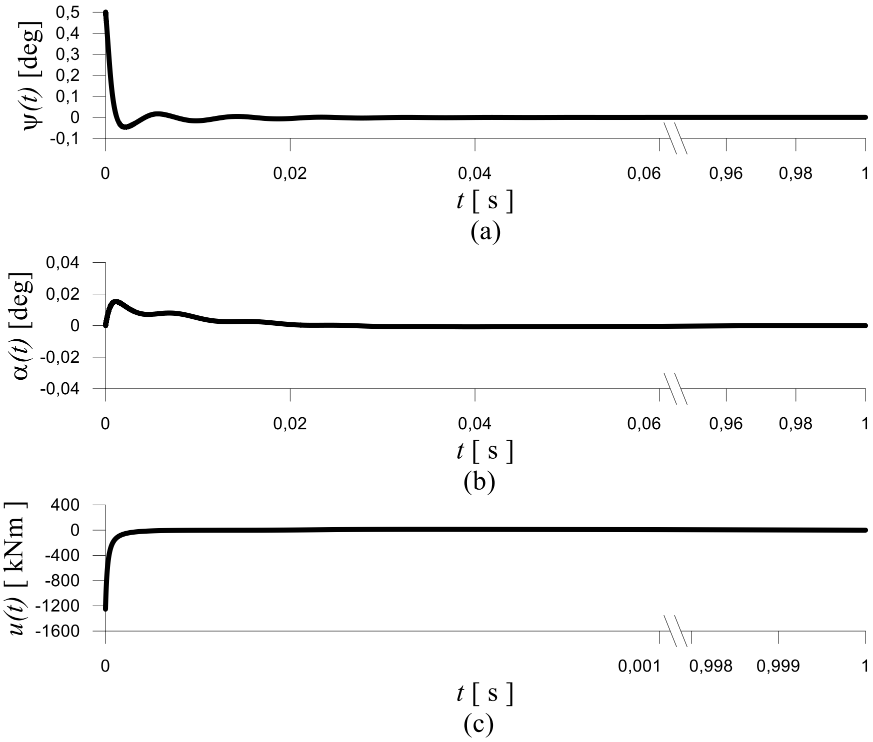

Fig. 7 Closed loop transient response without input saturation

elements (Limebeer and Massaro 2018), it is imperative that the shimmy oscillations are damped as fast as possible.

By simulating the transient response undergoing an initial disturbance ψ_0=0.5 deg and travelling at the critical speed, it is obtained that low values of the adaptive gains allow to obtain a too slow damping behavior. The adaptive gains are thus set as $\mathbf{\Gamma}_P = 10^7\, Nm/\deg^3$ and $\mathbf{\Gamma}_I = 10^8\, Nm/\deg^3 s$ moreover the integration constant of Eq. (4) is set to $K_{eI0} = 5\times 10^3\, Nm/\deg$ while the forgetting constant is set to $\eta = 10^{-3}\, s^{-1}$ in accordance with (Orlando 2020). Fig. 7 shows the time history of the fork-wheel rotation angle ψ, of the tire sideslip angle α and of the applied control torque M_c. It appears evident that both the shimmy and the sideslip angles time histories converges to zero in about 0.04 s which means that the shimmy vibration is damped fast. However, it is also evident that the requested torque to control the NLG shimmy is extremely high. The maximum moment value that is considered as feasible in this work is $M_{c,\max} = 2\, kNm$ (Pouly *et al.* 2011).

For this reason, the simulation is run again but this time the actuator saturation is modeled as well. Results given in Fig. 8 allow to see that the MSAC control system is capable of fast damping the shimmy oscillation and that the control torque saturate. The fork-wheel rotation angle oscillation is damped in about 0.02 s while the tire sideslip angle reaches a maximum value of about α=0.055 deg and its vibration is damped in about 0.06 s. Observing the control moment torque history it appears that input saturates three time in about 1 s. Then its response rapidly decreases towards zero in about 0.02 s. This behavior can be considered a drawback since it results

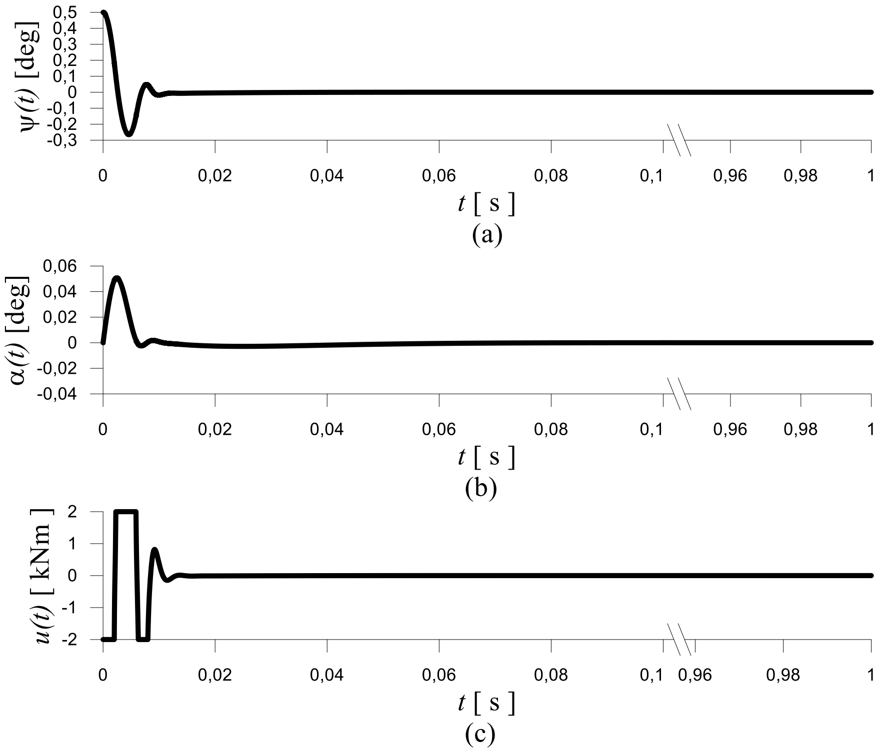

Fig. 8 Closed loop transient response with input saturation: V=20 m/s, ψ_0=0.5 deg

in an excessive load on the control actuator and can reduce its functionality and its life.

The response of the system is then investigated for increasing values of the initial disturbance and of the taxiing speed to study their effect on both the plant and the control actuator responses. It is obtained that at low values of the initial disturbance the main effect of the increasing velocity is to engender a greater tire sideslip angle during the initial transient. For instance, when ψ_0=0.5 deg the maximum tire sideslip angle increases as α={0.124, 0.22, 0.31, 0.36} deg when the advancing speed varies among V={20, 40, 60, 80} m/s. On the other hand, a higher value of the initial disturbance causes an increase of the number of saturated cycles of the actuator, as a consequence, the time needed to damp the shimmy vibration increases as well. In particular, when the taxiing speed becomes greater than 30 m/s and the initial disturbance is ψ_0=5 deg the actuation torque saturates oscillating between its maximum and minimum values; this engenders a windup in the system whose response now show limit cycle oscillations, see Fig. 9.

It can now be observed that the response of the controlled system is now alike the open-loop transient response, see Fig. 5(b), and the LCO amplitude is ψ_{LCO}=25.8 deg. This behavior is motivated by the fact that the saturated input signal is no longer influenced by the system output and thus the closed-loop system behaves as an open-loop one. An “engineering solutions” (Hippe 2006) is adopted to identify the state of the controlled system that is winding up during the input saturation and to solve such issue. In detail, it has been found that the windup is introduced into the system by the PFC which acts as a first order system applied to the MSAC control input signal, see Fig. 1. The adopted “engineering solutions” consists in the application of a simple back-calculation anti-windup (Hippe 2006) control mechanism having time constant T_{wup}=0.318 s. Fig.

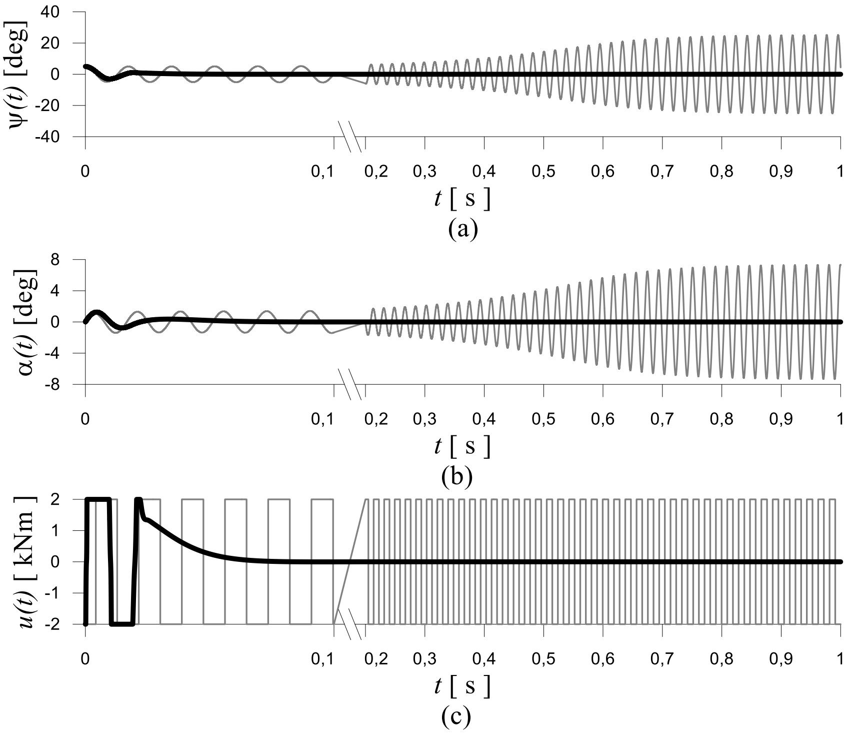

Fig. 9 Closed loop transient response with input saturation and anti-windup (black): V=30 m/s, ψ_0=5 deg

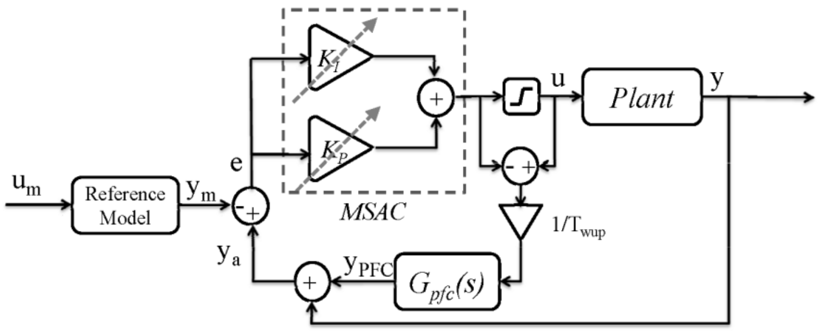

Fig. 10 PFC-MSAC scheme with saturation and Anti-Windup

10 the updated PFC-MSAC control scheme with anti-windup. Results obtained by using the anti-windup control mechanism are shown in Fig. 9. It appears that the presence of the anti-windup scheme allows the adaptive damping system to suppress the shimmy vibration in about 0.05 s.

A comparison with other controlling techniques is now studied with the aim of verifying the soundness of the proposed anti-windup PFC-MSAC scheme. The response of the proposed control scheme is compared with results obtained by using an anti-windup filtered PID (fPID) scheme previous proposed by the Authors in (Orlando and Alaimo 2017).

Results are also compared with transient data taken from literature (Kuntanapreeda 2018) where the tensor product model transformation (TPMT) is used, to account for linear variation of

Table 1 Comparison results

	t_s [s]	$\lvert\psi\rvert_{\max}$ [deg]	$\lvert u\rvert_{\max}$ [kNm]	$t_{u\text{-}sat}$ [s]
MSAC	0.035	3.015	2.00	0.023
fPID	0.091	4.423	2.00	0.046
TPMT	0.067	5.314	6.44	-

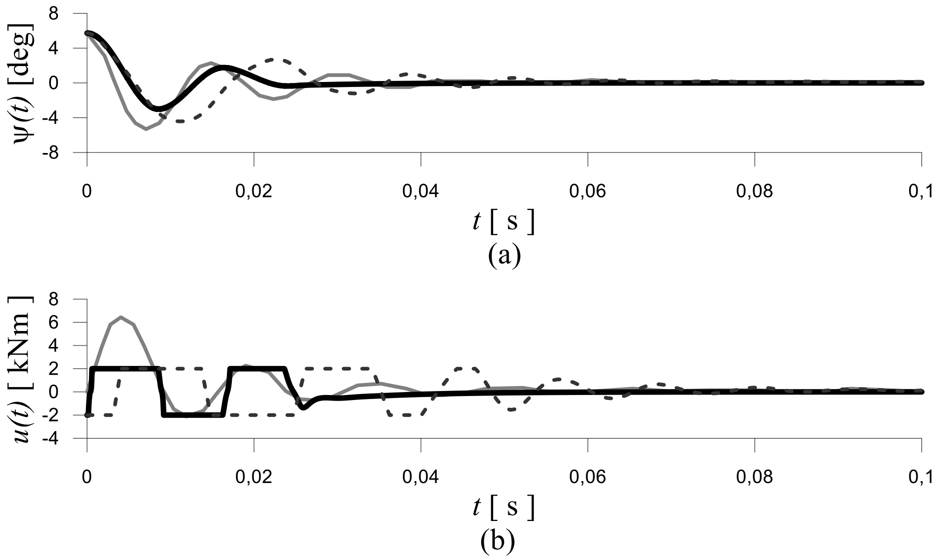

Fig. 11 Comparison of results obtained by MSAC (black), TPMT (grey) and fPID (dotted) controllers

the system's parameters, along with a parallel distributed compensation (PDC) controller to obtain an asymptotically stable closed loop system. In particular, to compare simulation results with data reported in literature (Kuntanapreeda 2018), it is assumed that the NLG is travelling with a speed of V=75 m/s, the caster length is set to e=0.3 m, the NLG damping constant is K_D=20 Nsm/rad. The remaining mechanical parameters are not changed with respect to previous analyzed cases and can be found in (Orlando and Alaimo 2017). The initial disturbance is set to ψ_0=5.73 deg. From Fig. 11 it can be observed that all the compared control schemes are able to reduce the shimmy vibration very fast despite the very large value of the initial disturbance. However, it can also be appreciated that the controlling torque $u(t)$ lead by the TPMT-PDC controller is higher than the limiting value $M_{c,max}$=2 kNm given in (Pouly *et al.* 2011). On the other hand, the input signals of both the MSAC and fPID closed loop systems present saturation but the anti-windup scheme allows the system to damp the shimmy oscillation. Table 1 shows comparison results in terms of settling time t_s, maximum value of the shimmy rotation $\lvert\psi\rvert_{\max}$ after the initial disturbance, maximum value of the controlling torque $\lvert u\rvert_{\max}$ and the time extent of input saturation $t_{u\text{-}sat}$. It can be noted that the proposed MSAC is able to dampen vibrations in less time by reaching smaller rotation angles. The saturation time is also reduced with respect to the fPID controller.

5. Conclusions

An adaptive control system has been proposed in the present work to damp the shimmy oscillation of the nose landing gear. The proposed controller takes advantage of the Modified Simple Adaptive Control theory that allows to control the NLG shimmy vibration by using only one output feedback variable. In order to meet the almost strictly passivity conditions of the controlled plant, a Parallel Feedforward Compensator has been introduced. Numerical simulations have been carried out to investigate both the open and closed loop results for different taxiing velocities and initial disturbances. To account for physical limitation of the controlling actuator, saturation limits have been modeled. For some velocity and initial disturbance conditions, numerical simulation have revealed the occurrence of windup. The issue has been coped for by implementing a back-propagation anti-windup mechanism to avoid such detrimental effect. Comparison with literature results have shown the soundness of the proposed anti-windup PFC-MSAC shimmy suppression control approach.

References

Alaimo, A., Esposito, A. and Orlando, C. (2019), "P$_D$SO tuning of PFC-SAC fault tolerant flight control system", *Adv. Aircraft Spacecraft Sci.*, **6**(5), 349-369. https://doi.org/10.12989/aas.2019.6.5.349.

Alaimo, A., Milazzo, A. and Orlando, C. (2016), "Nonlinear model based particle swarm optimization of PID shimmy damping control", *Adv. Aircraft Spacecraft Sci.*, **3**(2), 211-244. https://doi.org/10.12989/aas.2016.3.2.211.

Andrievsky, B., Kudryashova, E.V., Kuznetsov, N.V., Kuznetsova, O.A., Tomashevich, S. and Mokaev, T.N. (2019), "Simple adaptive control of aircraft roll angle, suppressing the wing rock oscillations", *Math. Eng. Sci. Aerosp.*, **10**(3), 373-386.

Andrievsky, B.R., Fradkov, A.L. and Kaufman, H. (1994), "Necessary and sufficient conditions for almost strict positive realness and their application to direct implicit adaptive control systems", *Proceedings of the 1994 American Control Conference-ACC'94*, Baltimore, Maryland, U.S.A., June-July.

Åström, K.J. and Wittenmark, B. (2013), *Adaptive Control*, Courier Corporation.

Barkana, I. (1987), *On Parallel Feedforward and Simplified Adaptive Control*, in *Adaptive Systems in Control and Signal Processing*, Pergamon Press, 99-104.

Barkana, I. (2005), "Classical and simple adaptive control for non-minimum phase autopilot design", *J. Guid. Control Dynam.*, **28**(4), 631-638. https://doi.org/10.2514/1.9542.

Barkana, I. (2014), "Simple adaptive control - a stable direct model reference adaptive control methodology - a brief survey", *Int. J. Adapt. Control. Signal Process*, **28**(7-8), 567-603. https://doi.org/10.3182/20070829-3-RU-4911.00049.

Barkana, I. and Kaufman, H. (1985), "Global stability and performance of a simplified adaptive algorithm", *Int. J. Control*, **42**(6), 1491-1505. https://doi.org/10.1080/00207178508933440.

Hippe, P. (2006), *Windup in Control: Its Effects and Their Prevention*, Springer Science & Business Media.

Kuntanapreeda, S. (2018), "Control of shimmy vibration in aircraft landing gears based on tensor product model transformation and twisting sliding mode algorithm", *Proceedings of the 13th International Scientific-Technical Conference on Electromechanics and Robotics "Zavalishin's Readings"*, St. Petersburg, Russia, April.

Lavretsky, E. and Wise, K.A. (2013), *Robust and Adaptive Control: With Aerospace Applications*, Springer.

Limebeer, D.J. and Massaro, M. (2018), *Dynamics and Optimal Control of Road Vehicles*, Oxford University Press.

Ma, Y., Cocquempot, V., El Najjar, M.E.B. and Jiang, B. (2017), "Multidesign integration based adaptive actuator failure compensation control for two linked 2WD mobile robots", *IEEE T. Mechatron.*, **22**(5), 2174-2185. https://doi.org/10.1109/TMECH.2017.2731523.

Matsuki, H., Nishiyama, T., Omori, Y., Suzuki, S., Masui, K. and Sato, M. (2018), "Flight test of fault-tolerant flight control system using simple adaptive control with PID controller", *Aircr. Eng. Aerosp. Tec.*, **90**(1), 210-218. https://doi.org/10.1108/AEAT-03-2016-0052.

Omori, Y., Suzuki, S. and Masui, K. (2013), "Flight test of fault-tolerant flight control system using simple adaptive control with PID compensator", *Proceedings of the AIAA Infotech@ Aerospace (I@ A) Conference*, Boston, Massachusetts, U.S.A., August.

Orlando, C. (2020), "Nose landing gear simple adaptive shimmy suppression system", *J. Guid. Control Dynam.*, **43**(7), 1298-1312, https://doi.org/10.2514/1.G004832.

Orlando, C. and Alaimo, A. (2017), "A robust active control system for shimmy damping in the presence of free play and uncertainties", *Mech. Syst. Signal Pr.*, **84**, 551-569. https://doi.org/10.1016/j.ymssp.2016.07.038.

Pacejka, H. (2005), *Tire and Vehicle Dynamics*, Elsevier.

Pouly, G., Huynh, T.H., Lauffenburger, J.P. and Basset, M. (2008), "Active shimmy damping using Fuzzy Adaptive output feedback control", *Proceedings of the 2008 10th International Conference on Control, Automation, Robotics and Vision*, Hanoi, Vietnam, December.

Pouly, G., Huynh, T.H., Lauffenburger, J.P. and Basset, M. (2011), "State feedback fuzzy adaptive control for active shimmy damping", *Eur. J. Control*, **17**(4), 370-393. https://doi.org/10.3166/ejc.17.370-393.

Rahmani, M. and Behdinan, K. (2019), "On the effectiveness of shimmy dampers in stabilizing nose landing gears", *Aerosp. Sci. Technol.*, **91**, 272-286. https://doi.org/10.1016/j.ast.2019.05.040.

Rusnak, I. and Barkana, I. (2009), "SPR and ASPR untangled", *IFAC Proc. Vol.*, **42**(6), 126-131. https://doi.org/10.3182/20090616-3-IL-2002.00022.

Sobel, K., Kaufman, H. and Mabius, L. (1979), "Model reference output adaptive control systemswithout parameter identification", *Proceedings of the 18th IEEE Conference on Decision and Control including the Symposium on Adaptive Processes*, Ft. Lauderdale, Florida, U.S.A., December.

Somieski, G. (1997), "Shimmy analysis of a simple aircraft nose landing gear model using different mathematical methods", *Aerosp. Sci. Technol.*, **1**(8), 545-555. https://doi.org/10.1016/S1270-9638(97)90003-1

Ulrich, S. and de Lafontaine, J. (2007), "Development of a novel adaptive control algorithm for a fighter aircraft", *Proceedings of the AIAA Guidance, Navigation and Control Conference and Exhibit*, Hilton Head, South Carolina, U.S.A., August.

Ulrich, S., Sasiadek, J.Z. and Barkana, I. (2012), "Modeling and direct adaptive control of a flexible-joint manipulator", *J. Guid. Control Dynam.*, **35**(1), 25-39. https://doi.org/10.2514/1.54083.

CC